Journal of Mechatronics Engineering

# PARACONSISTENT LOGIC APPROACH FOR ACTIVE NOISE REDUCTION

ARNALDO DE CARVALHO JUNIOR[1],
JOÃO FRANCISCO JUSTO FILHO[2], ALEXANDRE MANIÇOBA DE OLIVEIRA[1],
CHARLES ARTUR SANTOS DE OLIVEIRA[1], JOÃO INACIO DA SILVA FILHO[3]

[1]Federal Institute of São Paulo (IFSP), Maxwell Laboratory
[2] University of São Paulo (USP), Microelectronics Laboratory
[3]Santa Cecília University (UNISANTA)

<adecarvalhojr@ifsp.edu.br>,
<jjusto@lme.usp.br>, <amanicoba@ifsp.edu.br>,
<charles@ifsp.edu.br>, <inacio@unisanta.br>
DOI: 10.21439/jme.v3i1.81

**Received:** 16 Mar. 2019. **Accepted:** 02 Apr. 2019

**Abstract.** The Active Noise Reduction (ANR) is widely used in aircraft, headsets, telecommunications and medicine systems, to reduce or eliminate noise, while maintaining the characteristics of the desired signal. In this article a network of paraconsistent artificial neural cells (PANC) will be presented, based on the paraconsistent annotated logic by 2 values annotations (PAL2v) that allows to operate as ANR. Simulations indicate that the results presented by $\text{ANR}_{PAL}$ are better than those obtained by classic filters.

**Keywords:** ANR, Noise, PAL2v, PANC, $\text{PANCL}_{CTX}$

## 1 Introduction

The active noise reduction (ANR), also called noise cancellation (Noise Cancellation – NC) or Active Noise Control (ANC) occurs when a system is able to reduce an unwanted signal (noise, for example) by adding a second signal, which cancels the first (ASLAM; SHI; LIM, 2019). ANR has several applications, such as for noise reduction in the passenger cabin of the aircraft, air conditioning ducts, incubators for magnetic resonance systems, sensors in the human body, telecommunications, among others (ASLAM; SHI; LIM, 2019). An algorithm is used in the ANR to actively analyze and filter samples of the output signal and combine it with the input signal, in order to reduce noise, without destroying the desired input signal information (KUO; MORGAN, 1999). A generic block diagram is shown in Figure 1.

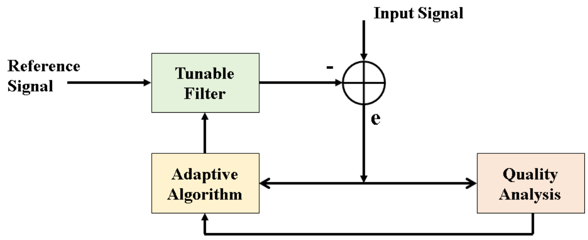


**Figure 1:** Diagram for active noise reducer. Source: Aslam, Shi e Lim (2019).

The paraconsistent annotated logic with two values annotation (PAL2v), as well as the other variations of the paraconsistent logic, repeals the principle of non-contradiction of classical logics, instead, it accepts contradictions in its theoretical structure, allowing to treat signals contaminated by uncertainties (MINICZ et al., 2014).

Paraconsistent artificial neural cells (PANC) can be built based on the PAL2v definitions and equations, which when combined, can form paraconsistent analysis networks (PAN) (ABE, 2004). This article explores the inherent characteristics of PAL2v and the application of two PANC, called PANCS (standard) and PANCL$_{CTX}$ (PANC of learning by contradiction effects extraction) to compose in Matlab® Simulink a noise reducing ANR block, with promising results in comparison to classical filters.

## 2 Paraconsistent Artificial Neural Cells

In PAL2v, through a pair of values ($\mu_1$, $\mu_2$) normalized between [0,1], are used to express knowledge about a proposition P ($\varepsilon\tau$) in a Lattice diagram. The extreme limits of the diagram are $\tau$ - True, $F$ - False, $T$ - Inconsistent and $\perp$ - Undetermined, as presented in Figure 2.

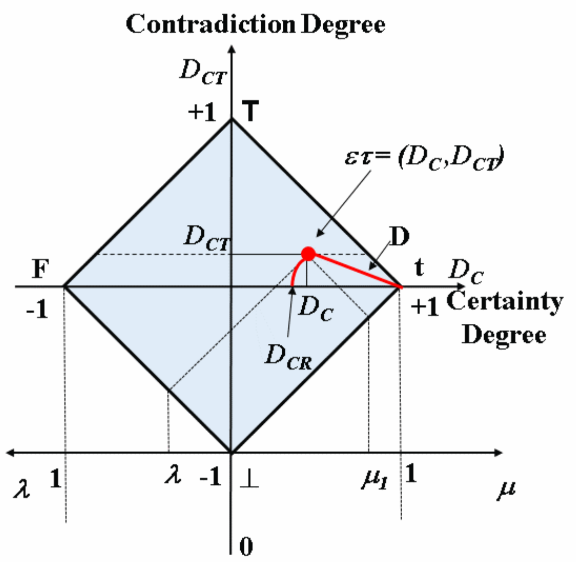


**Figure 2:** Lattice Diagram of PAL2v. Source: Adapted of Coelho et al. (2019).

The basic mathematic involved with PAL2v is presented by Equations (1) to (6).

$$\lambda = 1 - \mu_2 \quad (1)$$

$$D_C = \mu - \lambda \quad (2)$$

$$D_{CT} = \mu + \lambda - 1 \quad (3)$$

$$\mu_E = \frac{D_C + 1}{2} + \frac{\mu - \lambda + 1}{2} \quad (4)$$

$$\mu_{ECT} = \frac{D_{CT} + 1}{2} = \frac{\mu + \lambda - 1 + 1}{2} = \frac{\mu + \lambda}{2} \quad (5)$$

$$\varphi_E = 1 - [D_{CT}] \quad (6)$$

The input $\mu$ or $\mu_1$ represents the degree of favorable evidence. The complement of the second entry ($\mu_2$), calculated in Equation (1), is called degree of unfavorable evidence ($\lambda$). The resulting degree of evidence ($\mu E$), calculated in Equation (4), corresponds to the degree of certainty ($D_C$), in the Lattice diagram, normalized between [0,1]. The degree of real certainty ($D_{CR}$) is the projection of the line $D$ over the certainty axis, as indicated in Figure 2, is used in this document. The resulting degree of contradiction ($\mu_{ECT}$) corresponds to the degree of contradiction ($D_{CT}$) normalized between [0,1]. The certainty interval ($\varphi_E$) can be calculated as Equation (4).

The PANCS is composed by a block of code containing the equations and interpretations of PAL2v written in the form of an algorithm. The symbol of this cell is presented in Figure 3(a) (CARVALHO JUNIOR et al., 2018) (CARVALHO JUNIOR; SILVA FILHO; MARIO, 2018), whose mathematical representation is presented in Equation (4) and (5).

By applying the complement of the output ($1 - \mu_E$) back to the input of degree of unfavorable evidence ($\lambda$), it is possible to create the PANCL (PANC of learning) that has this name because the output tends to follow the input $\mu$ with a certain delay (CARVALHO JUNIOR et al., 2018). The PANCL$_{CTX}$ is a variation of PANCL, first presented in (MINICZ et al., 2014), whose symbol is presented in Figure 3(b).

As in PANCL, the current output is complemented and applied to the input ($\lambda$). A learning factor ($F_L$) is used to accelerate or delay the cell's performance. As shown in (CARVALHO JUNIOR et al., 2018), the $\mu_E$ output of this cell can act as an integrator, while the $\mu_{ECT}$ output can act as a derivative (CARVALHO JUNIOR; SILVA FILHO; MARIO, 2018). The PANCLCTX can be built from the PANCS as presented in Figure 4. Equation (7) presents the $\mu_E$ output of PANCL$_{CTX}$ (MINICZ et al., 2014). By mathematical development, it can be proved that Equation (8) evolves to that presented in (7).

$$\mu_E\,[n] = \mu_E\,[n-1] + F_L \times D_{CT} \quad (7)$$

$$\mu_E\,[n] = (1 - F_L) \times \mu_E\,[n-1] + F_L \times \mu\,[n] \quad (8)$$

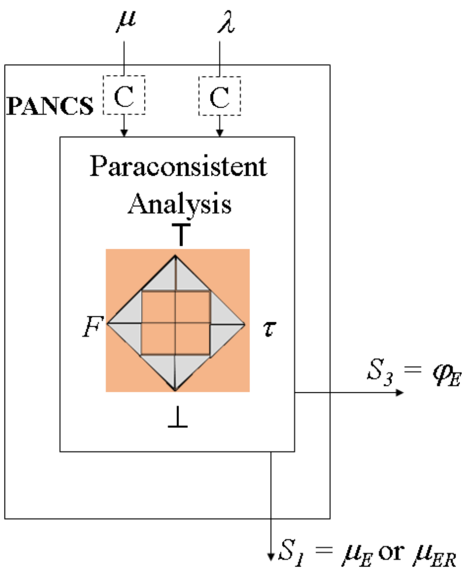


(a)

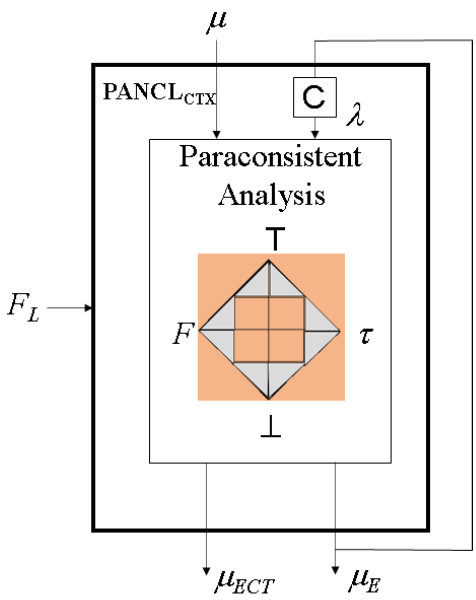


(b)

**Figure 3:** PANCS symbol (a) and PANCL$_{CTX}$ symbol (b).
Source: Adapted of (CARVALHO JUNIOR et al., 2018).

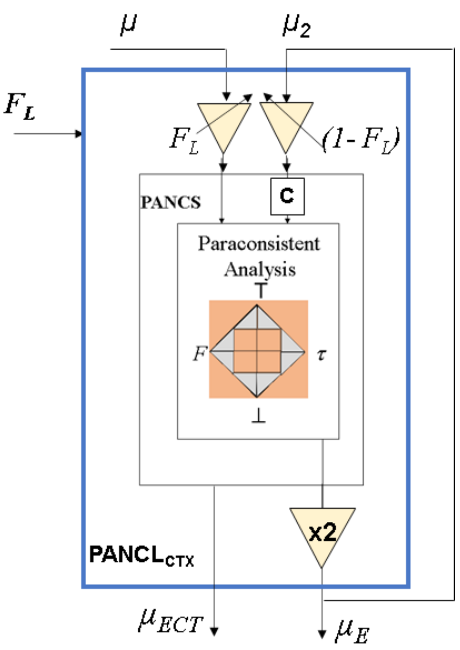


**Figure 4:** PANCL$_{CTX}$ construction.

Similarly, it is possible to prove that Equation (5) evolves to (9), as equation of differences, in order to find $\mu_{ECT}$ output. The PANCL$_{CTX}$ can be applied as an estimator or in the treatment and filtering of signals, as presented in (CARVALHO JUNIOR et al., 2018; CARVALHO JUNIOR; SILVA FILHO; MARIO, 2018).

$$\begin{aligned} \mu_{ECT}[n] = (1 - F_L) \times (\mu_{ECT}[n-1] - 0.5) \\ +0.5 \times (\mu[n] - \mu[n-1]) + 0.5 \end{aligned} \tag{9}$$

## 3 Methodology

The PANCS and PANCL$_{CTX}$ models are built in Matlab® Simulink for the simulations, as presented in Figure 5.

The basic structure of an active noise reduction unit using PAL2v, called as Paraconsistent Active Noise Reducer (ANR$_{PAL}$), is presented in Figure 6.

The signal contaminated by noise, after being normalized between [0,1], centered at 0.5 level, is applied simultaneously to the input of favorable evidence ($\mu$) of a PANCL$_{CTX}$ and a PANCS. If the peak-to-peak amplitude of the signal plus input noise exceeds the range [0,1] it must be attenuated before being applied to the

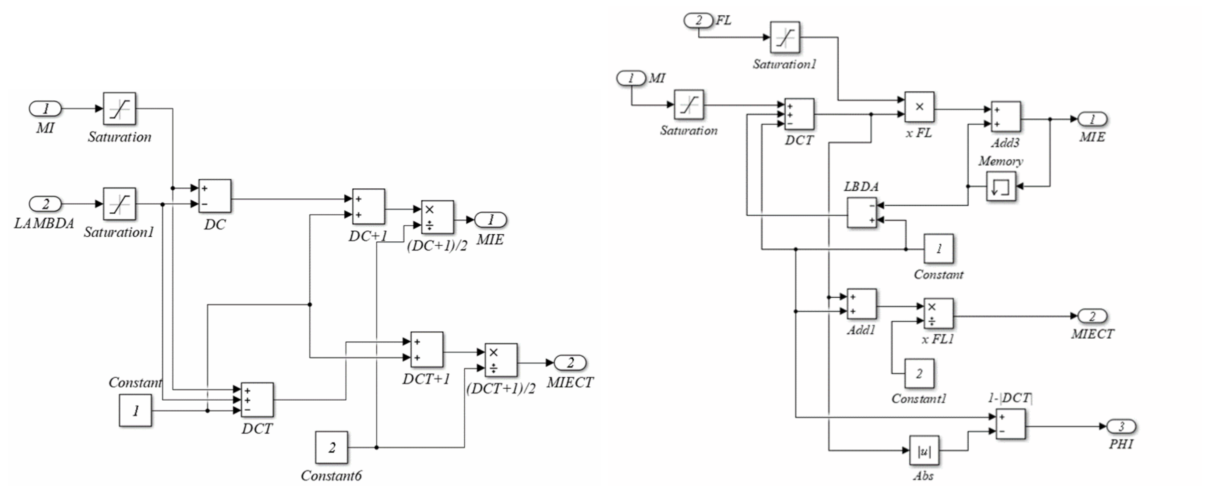


(a) (b)

**Figure 5:** PANCS (a) and PANCL$_{CTX}$ (b) as built in Simulink.

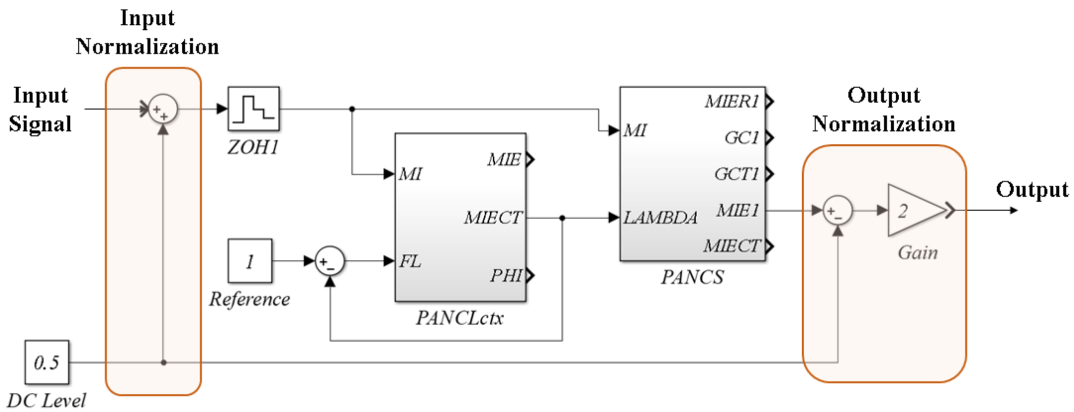


**Figure 6:** PANCS (a) and PANCL$_{CTX}$ (b) as built in Simulink.

ANR$_{PAL}$ input, in order to guarantee the consistency with the PAL2v logic. The PANCL$_{CTX}$ $\mu_{ECT}$ output is used to separate the noise from the signal. The noise now is applied to the PANCS unfavorable evidence level ($\lambda$) entry. The output of the PANCS, presents a signal similar to the one applied to the input, with a reduction in the amplitude of the noise, maintaining the original characteristics of the desired signal. At the output of the ANR$_{PAL}$, the signal is normalized back to the original amplitude. A more elegant solution uses interval of certainty ($\varphi_E$) instead of $D_{CT}$, with the same results, as presented in Figure 7. The reason is that the certainty interval considers the module of the contradiction degree, according to the Equation (6).

The connection of ANR$_{PAL}$ blocks in cascade allows to increase the signal-to-noise ratio (SNR) of the system, according to simulations performed with different input patterns via MATLAB SIMULINK. Note that the $\mu_{ECT}$ output of PANCL$_{CTX}$ is complemented and applied back to the $F_L$ (Cell Learning Factor) input. In this way, rapid peaks of noise cause the cell to respond slowly, while low peaks, it responds more quickly. This brings an adaptability to the ANR$_{PAL}$ block. The results of ANR$_{PAL}$ are also compared to a low pass PAL2v Filter presented in (CARVALHO JUNIOR et al., 2018), made of 3 PANCL$_{CTX}$ in cascade. The results of the simulations are presented in the next section.

## 4 Results and Discussion

For the simulations, sinusoidal input signal of 0.2 Vpp, 100 and 1000 Hz are used. The compared results between PAL2v filter (CARVALHO JUNIOR et al., 2018) using 3 cells and the ANR$_{PAL}$ also with 3 modules, at 100 Hz, is presented in Figure 8(a). Another results at 1000 Hz is presented in Figure 8(b).

The sampling rate of 0.4 msec is used. The noise power of the "band-limited white noise" object of the Simulink Tool is 0.2x10$^{-6}$. In low frequencies and high sampling time, the PAL2v filter works well. But note that as the frequency increases, the PAL2v filter eliminates noise, but presents an attenuation and add a delay to the desired signal, since it is dependent on the $F_L$ parameter and the sampling rate used (red line), whereas ANR$_{PAL}$ (line blue) follows the characteristics of the desired signal in both figures.

The Bode diagram relative to the ANR$_{PAL}$ is presented in Figure 9. The limitation is the sampling rate used. Note that it has a flat response up to the limit of the sampling rate used. At 10 kHz, the magnitude only -0.075 dB.

The Bode diagram relative to PAL2v filter with 3 cells in cascade for the same scenario is presented in Figure 10. Compared to Figure 9, the filter using $F_L$ of 0.5 (color blue) presented a cutoff frequency at 8.67 kHz, the filter using $F_L$ equal to 0.25 presented the cutoff frequency at 3.55 kHz and the filter using $F_L$ equal to 0.1 presented the cutoff frequency at 1.3 kHz.

The Table 1 presents the SNR results for 1 to 4 cascading ANR$_{PAL}$ blocks. The rightmost column of table 1 shows the combined result of 1 PANCL$_{CTX}$ cell working as low pass filter at the input of a 4-module ANR$_{PAL}$. The gain of the normalizer output must be $2n$, where $n$ is the number of ANR$_{PAL}$ blocks.

**Table 1:** Results for 1 to 4x ANR$_{PAL}$ blocks in cascade.

| Input (Hz) | SNR (dB) | 1x ANR$_{PAL}$ (dB) | 2x ANR$_{PAL}$ (dB) | 3x ANR$_{PAL}$ (dB) | 4x ANR$_{PAL}$ (dB) | 1x PAL2v Filter + 4x ANR$_{PAL}$ (dB) |
|---|---|---|---|---|---|---|
| 100 | 15.26 | 20.10 (+4.84) | 22.78 (+7.52) | 24.3 (+9.04) | 25.27 (+10.01) | 25.98 (+10.72) |
| 1000 | 16.05 | 20.97 (+4.92) | 23.78 (+7.73) | 25.36 (+9.31) | 26.37 (+10.32) | 27.09 (+11.03) |

## 5 Conclusion

In this study, an active noise reduction system using few paraconsistent artificial neural cells (ANR$_{PAL}$), based on PAL2v, is presented. The noise reduction did not reflect changes in the characteristics of the desired signal. Other combinations of PANC can be experimented in order to seek a higher signal-to-noise ratio, without affecting the desired signal. The combined performance of ANR$_{PAL}$ with PAL2v Filter can also be tried. The PAL2v used in this article have a low mathematical complexity, which allows their implementation in embedded systems while consuming little computational resources.

## Acknowledgement

The authors would like to thank the Polytechnic School of the Universidade de São Paulo for the software tools used in this article.

## References

ABE, J. M. Paraconsistent artificial neural networks: An introduction. In: SPRINGER. **International Conference on Knowledge-Based and Intelligent Information and Engineering Systems**. New Zealand, 2004. p. 942–948.

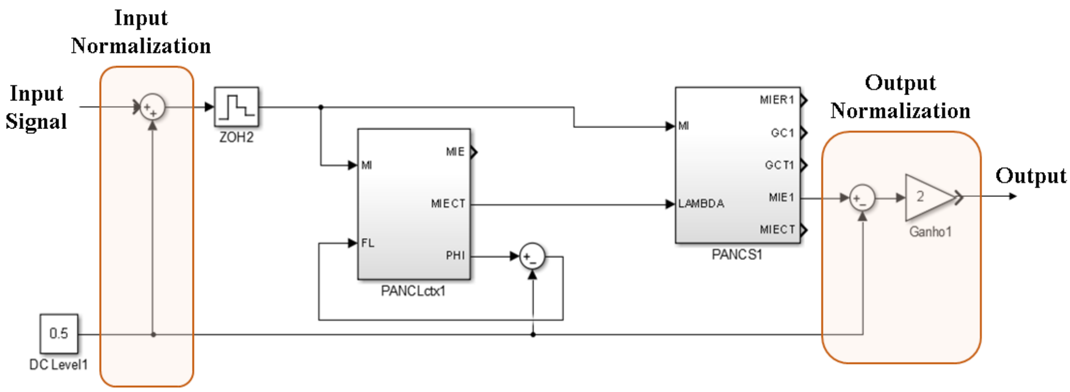


**Figure 7:** Basic paraconsistent ANR using $\varphi_E$ instead of $D_{CT}$.

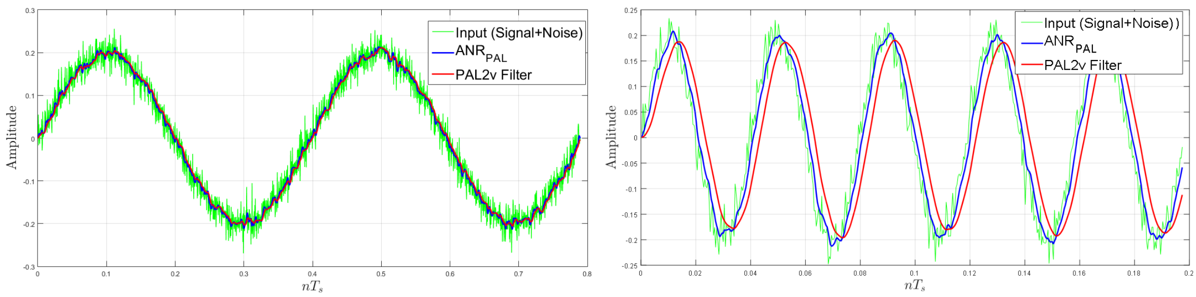


(a) (b)

**Figure 8:** Comparison of the signal + noise applied to the input (green) and the output of 3x ANR$_{PAL}$ (blue) and 3x PAL2v Filter (red) using FL of 0.25 at 100 Hz(a) and at 1000 Hz (b).

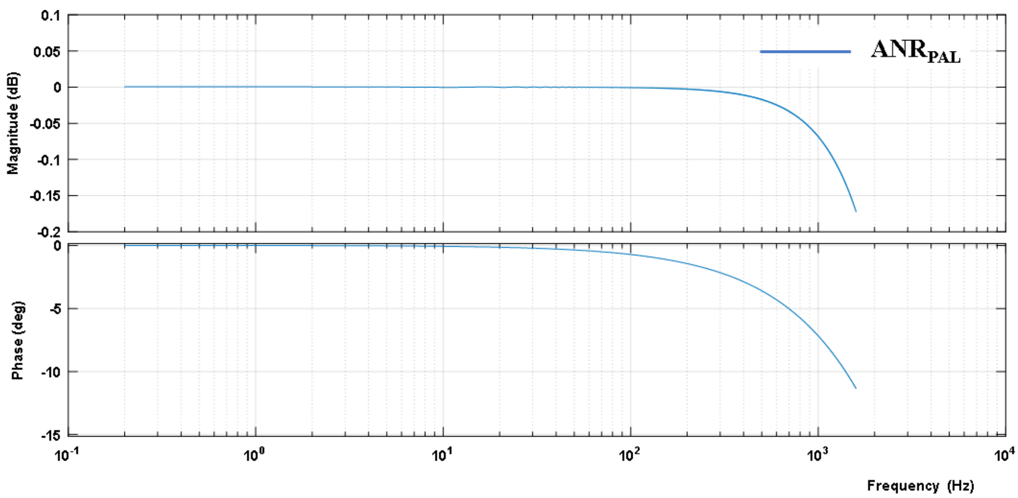


**Figure 9:** Bode diagram of ANR$_{PAL}$ with 3 blocks in cascade.

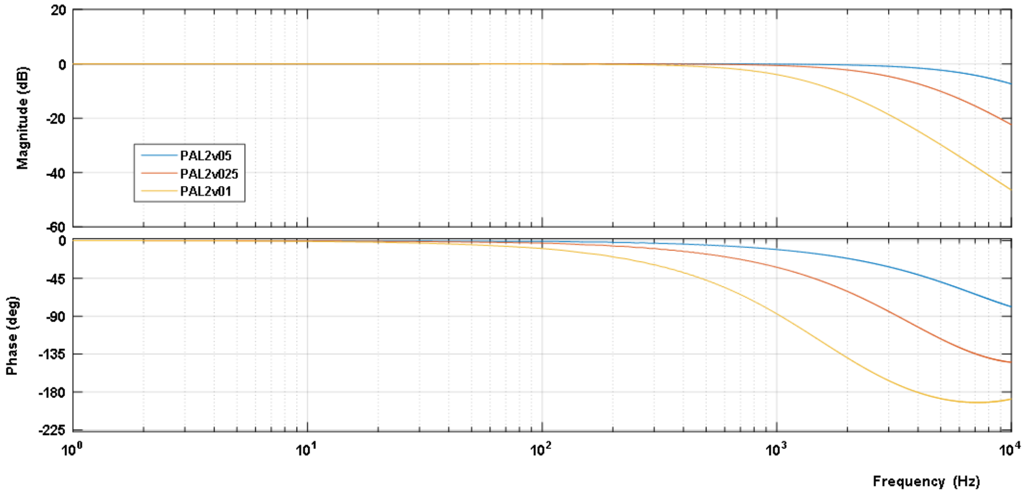


**Figure 10:** Bode diagram of PAL2v Filter with 3 cells in cascade.

ASLAM, M. S.; SHI, P.; LIM, C.-C. Robust active noise control design by optimal weighted least squares approach. **IEEE Transactions on Circuits and Systems I: Regular Papers**, IEEE, v. 66, n. 10, p. 3955–3967, 2019.

CARVALHO JUNIOR, A.; FILHO, J. I. D. S.; MARIO, M. C.; BLOS, M. F.; CRUZ, C. M. da. A study of paraconsistent artificial neural cell of learning applied as pal2v filter. **IEEE Latin America Transactions**, IEEE, v. 16, n. 1, p. 202–209, 2018.

CARVALHO JUNIOR, A.; SILVA FILHO, J. I.; MARIO, M. C. Estimador de estado adaptativo paraconsistente. **Exatas Online**, v. 9, n. 1, p. 25–30, 2018.

COELHO, M. S.; FILHO, J. I. da S.; CÔRTES, H. M.; JR, A. de C.; BLOS, M. F.; MARIO, M. C.; ROCCO, A. Hybrid pi controller constructed with paraconsistent annotated logic. **Control Engineering Practice**, Elsevier, v. 84, n. 1, p. 112–124, 2019.

KUO, S. M.; MORGAN, D. R. Active noise control: a tutorial review. **Proceedings of the IEEE**, IEEE, v. 87, n. 6, p. 943–973, 1999.

MINICZ, M. d. F.; MATUCK, G.; TASINAFFO, P.; FILHO, J. D. S. Célula neural artificial paraconsistente de aprendizagem por extração do efeito da contradição. **Revista Seleção Documental**, v. 1, n. 33, p. 3–9, 2014.